



Loh, S. Y., Jahans-Price, T., Greenwood, M. P., Greenwood, M., Hoe, S. Z., Konopacka, A., Campbell, C., Murphy, D., & Hindmarch, C. C. T. (2017). Unsupervised network analysis of the plastic supraoptic nucleus transcriptome predicts caprin2 regulatory interactions. *eNeuro*, 4(6), [e0243-17.2017].
<https://doi.org/10.1523/ENEURO.0243-17.2017>

Publisher's PDF, also known as Version of record

License (if available):
CC BY

Link to published version (if available):
[10.1523/ENEURO.0243-17.2017](https://doi.org/10.1523/ENEURO.0243-17.2017)

[Link to publication record in Explore Bristol Research](#)
PDF-document

This is the final published version of the article (version of record). It first appeared online via Society for Neuroscience at <http://www.eneuro.org/content/4/6/ENEURO.0243-17.2017> . Please refer to any applicable terms of use of the publisher.

University of Bristol - Explore Bristol Research

General rights

This document is made available in accordance with publisher policies. Please cite only the published version using the reference above. Full terms of use are available:
<http://www.bristol.ac.uk/red/research-policy/pure/user-guides/ebr-terms/>

Integrative Systems

Unsupervised Network Analysis of the Plastic Supraoptic Nucleus Transcriptome Predicts *Caprin2* Regulatory Interactions

 Su-Yi Loh,^{1,†} Thomas Jahans-Price,^{2,†} Michael P. Greenwood,² Mingkwan Greenwood,² See-Ziau Hoe,¹ Agnieszka Konopacka,²  Colin Campbell,^{3,#}  David Murphy,^{1,2,#} and  Charles C. T. Hindmarch^{1,4,#}

DOI:<http://dx.doi.org/10.1523/ENEURO.0243-17.2017>

¹Department of Physiology, Faculty of Medicine, University of Malaya, Kuala Lumpur 50603, Malaysia, ²School of Clinical Sciences, University of Bristol, Bristol BS1 3NY, United Kingdom, ³Department of Engineering Mathematics, University of Bristol, Bristol BS8 1UB, United Kingdom, and ⁴Queen's Cardiopulmonary Unit (QCPU), Translational Institute of Medicine (TIME), Department of Medicine, Queen's University, Kingston, Ontario, ON K7L 3N6 Canada

Abstract

The supraoptic nucleus (SON) is a group of neurons in the hypothalamus responsible for the synthesis and secretion of the peptide hormones vasopressin and oxytocin. Following physiological cues, such as dehydration, salt-loading and lactation, the SON undergoes a function related plasticity that we have previously described in the rat at the transcriptome level. Using the unsupervised graphical lasso (Glasso) algorithm, we reconstructed a putative network from 500 plastic SON genes in which genes are the nodes and the edges are the inferred interactions. The most active nodal gene identified within the network was *Caprin2*. *Caprin2* encodes an RNA-binding protein that we have previously shown to be vital for the functioning of osmoregulatory neuroendocrine neurons in the SON of the rat hypothalamus. To test the validity of the Glasso network, we either overexpressed or knocked down *Caprin2* transcripts in differentiated rat pheochromocytoma PC12 cells and showed that these manipulations had significant opposite effects on the levels of putative target mRNAs. These studies suggest that the predicative power of the Glasso algorithm within an *in vivo* system is accurate, and identifies biological targets that may be important to the functional plasticity of the SON.

Key words: *Caprin2*; functional plasticity; gene network; Glasso; supraoptic nucleus; transcriptome

Significance Statement

The scale and complexity of transcriptome datasets makes the identification of suitable targets for physiologic studies a daunting problem. Using the unsupervised graphical lasso (Glasso) algorithm, we reconstructed a putative network from 500 plastic genes in the supraoptic nucleus (SON) of the hypothalamus. The most active nodal gene identified within the network encodes RNA-binding protein CAPRIN2. We tested the validity of the Glasso network by either overexpressing or knocking down *Caprin2* transcripts in differentiated rat pheochromocytoma cells and showed that these manipulations had opposite effects on the levels of putative target mRNAs. Our studies suggest that the predicative power of the Glasso algorithm can identify biological targets that may be important in a *Caprin2* gene network mediating functional plasticity in the SON.

Received July 12, 2017; accepted September 25, 2017; First published November 30, 2017.

The authors declare no competing financial interests.

Author contributions: C.C.T.H., T.J.-P., D.M., and C.C. designed research; S.-Y.L., T.J.-P., M.G., M.P.G., S.-Z.H., and A.K. performed research; C.C.T.H., T.J.-P. analyzed data; D.M., M.G., M.P.G., and C.C.T.H. wrote the paper.

Introduction

The supraoptic nucleus (SON) of the mammalian hypothalamus is a central neuroendocrine integrative structure consisting of large magnocellular neurons (MCNs) whose axons project to the posterior lobe of the pituitary (PP; Burbach et al., 2001), a neurovascular interface through which the brain regulates peripheral organs to maintain homeostasis (Murphy et al., 2016). The SON is responsible for the synthesis of the neuropeptide hormones arginine vasopressin (AVP), which cleaved from its precursor propeptide *en route* from the SON to the PP (Murphy et al., 2016). On release, AVP travels through the blood stream to specific receptor targets located in the kidney where it promotes water reabsorption in the collecting duct (Breyer and Ando, 1994).

Lactation and dehydration evoke a dramatic remodeling of the SON (Hatton, 1997; Theodosis et al., 1998). A plethora of changes in morphology, electrical properties and biosynthetic and secretory activity have all been described (Sharman et al., 2004). For example, as a consequence of the depletion of pituitary stores that accompanies chronic osmotic stimulation, there is a need to synthesize more AVP. This starts with an increase in transcription (Murphy and Carter, 1990), which results in an increase in the abundance of both precursor hnRNAs (Kondo et al., 2004) and mature AVP mRNAs (Sherman et al., 1986). In addition, it has been demonstrated that the AVP mRNAs are subject to post-transcriptional modification in the form of an increase in the length of the 3' poly(A) tail following dehydration (Carrazana et al., 1988; Zingg et al., 1988; Carter and Murphy, 1989; Murphy and Carter, 1990). Recently, microarrays have been used to document transcriptome-wide changes in gene expression in the SON of male rats subject to salt-loading and dehydration (Hindmarch et al., 2006; Greenwood et al., 2015), and in female rats in response to both dehydration and 11 d of lactation (Qiu et al., 2011), and it has been suggested that these changes are part of an organized response to main-

taining homeostasis in a changing environment (Hindmarch et al., 2013).

The analysis pipeline for these, and indeed most microarray experiments, is one of normalization and statistical testing before the filtering according to some arbitrary cutoff, such as fold-change. The resulting list of transcripts can then either be mined manually to select well-regulated targets, or subjected to one of the many approaches to bioinformatic analysis according to gene function or pathway. While these strategies are well used and often return important findings, they are at odds with the unbiased philosophy behind the transcriptome-wide experiment, as they require that the target gene has already been described, typically in a tissue discrete from that under interrogation. To investigate new strategies for target prioritization, we have here employed network reconstruction/inference strategies to our SON microarray data in either the control state or the "plastic" state to test whether this is an effective strategy for the robust identification of important plastic genes in this tissue.

Network inference is a strategy whereby a network structure is estimated from transcriptome data; genes are the nodes of this network and the edges are the inferred interactions. Two main strategies exist when attempting to reconstruct gene networks. The most tractable approach uses supervised inference where a set of "known" links and non-links between genes are used as a training set to construct a classifier or decision function. This classifier can be subsequently used to estimate links or non-links between further nodes in a network. In the second approach, unsupervised inference is used and the network structure is assumed only from the transcriptome data presented and thus the inference problem is harder. Here, we use the unsupervised graphical lasso (Glasso) algorithm (Friedman et al., 2008) to generate a putative gene network (see Materials and Methods for a full description). Gene features in Glasso are viewed as nodes in a network that predicts stable and reproducible dependencies between these nodes. To validate the results from the Glasso algorithm, we inferred a second network model based on the matrix of Pearson correlation coefficients between nodes.

From the derived Glasso network, we identified a hub nodal gene, *Caprin2*, that encodes an RNA-binding protein that we have previously identified as being important in the central osmotic defense response (Konopacka et al., 2015). To test this prediction from the Glasso algorithm, we perturbed the network *in vitro* by manipulating *Caprin2* expression. We show that the predictive power of the Glasso algorithm is accurate and identifies genes that may be important in biological transitions.

Materials and Methods

Microarray data preparation

We re-mined raw data taken from analysis of 29 Affymetrix 230 2.0 microarrays that represented animals in either the naïve state ($n = 4$ female and $n = 5$ male) or the plastic state ($n = 5$ dehydration-male, $n = 5$ lactation-female, $n = 5$ dehydrated-female, $n = 5$ salt-loaded-male; Hindmarch et al., 2006; Qiu et al., 2011; Greenwood et al.,

This work was supported by the Medical Research Council (MRC) Grant MR/N022807/1 (to M.G. and D.M.); Biotechnology and Biological Sciences Research Council (BBSRC) Grants BB/G006156/1 (to A.K., M.P.G., and D.M.), BB/J005452/1 (to C.C.T.H. and D.M.), and BB/J015415/1 (to M.G. and D.M.); the Engineering and Physical Sciences Research Council (EPSRC) Grant EP/K008250/1 (to C.C. and D.M.); the British Heart Foundation (BHF) Grant RG/11/28714 (to M.P.G. and D.M.); the Wellcome Trust ISSF-Postdoctoral Research Staff Award 097822/Z/11/Z (to A.K.); the University of Cardiff (A.K.); and by High Impact Research Chancellory (UM.C/625/1/HIR/MOHE/MED/22 H-20001-E000086; to S.-Z.H., D.M., and C.C.T.H.) and Internationalisation Research (RP011-13HTM; to S.-Y.L., D.M., C.C.T.H.) grants from the University of Malaya.

[†]S.L. and T.J.P. are joint first authors.

[#]C.C., D.M., and C.C.T.H. are joint senior authors.

T. Jahans-Price's present address: Department of Experimental Psychology, University of Oxford, Oxford OX1 3UD, United Kingdom.

Correspondence should be addressed to either of the following: David Murphy at the above address, E-mail: d.murphy@bristol.ac.uk; or Charles C. T. Hindmarch at the above address, E-mail: chipboy101@gmail.com.

DOI: <https://doi.org/10.1523/ENEURO.0243-17.2017>

Copyright © 2017 Loh et al.

This is an open-access article distributed under the terms of the Creative Commons Attribution 4.0 International license, which permits unrestricted use, distribution and reproduction in any medium provided that the original work is properly attributed.

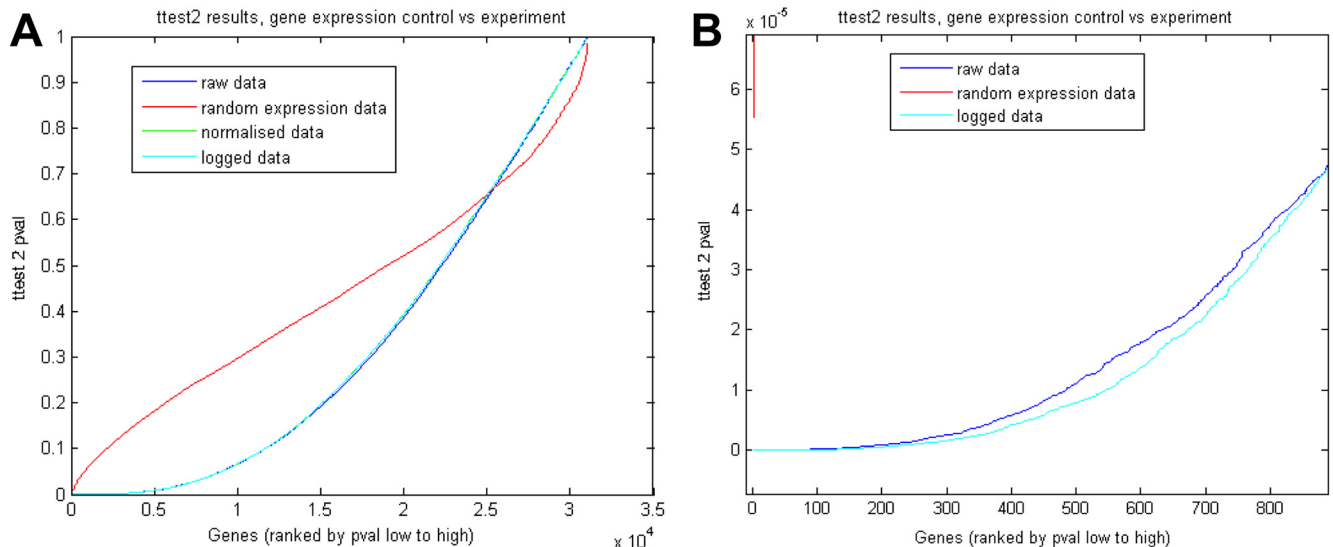


Figure 1. **A**, Microarray data t test, control versus experiment, genes ranked by $ttest2$ p value low to high. Raw data, normalized data, and logged data all gave comparable results. Randomly generated data gave higher p values for over half the gene pairs. Above the point of curve intersection microarray data stopped providing information, as significance was equivalent to randomly generated data. **B**, Zoomed in version of **A**, showing that the microarray data generated far lower p values compared to the random data. The lowest p value from randomly generated data were 1.5×10^{-5} . The figure shows that the top 500 genes are under 1×10^{-5} .

2015). NCBI Accession numbers (incorporating controls): male dehydration, GSE3110; male salt loading, GSE65663; female dehydration and lactation, GSE30733. We note that the biological importance of salt and water balance, especially after challenge, ensures small standard deviations (10%) in the data (Hindmarch et al., 2013). Validation using quantitative reverse transcription PCR (qRT-PCR; Hindmarch et al., 2006; Qiu et al., 2011; Greenwood et al., 2015; Fig. 3) has shown that the microarray data are very robust and reliable. We note that the genes encoding the two major neuropeptide products of the SON, AVP and oxytocin, are not represented in our differentially expressed gene list. The expression level of both these important peptides was so high within the control data that the signal was saturated, precluding any detection of upregulation following dehydration, lactation or salt loading (Hindmarch et al., 2006).

Initially trying to run Glasso on the entire SON microarray dataset of 31042 genes was prohibitive as a covariance matrix of 31042×31042 genes was too large to be stored in memory in R. Also, it is worth noting that many genes, even if well correlated with each other, were of lower interest as they are not necessarily strongly up or down regulated from control to experimental state. Therefore, it was necessary to reduce the size of the datasets to a manageable subset that only included potentially interesting genes, those that were significantly regulated between naïve and plastic states. To avoid the false discovery rate inherent in comparisons with sets of large numbers, we used a two-sample t test, comparing our experimental data against sets of 29 randomly generated matrices (using a Gaussian random deviate) of the same dimensionality (31042×31042 ; Fig. 1A). We performed a set of 10 such comparisons, against different sets of randomly generated matrices, and the most significant t test p values from this study were of order 10^{-5} , the most

significant p value from a comparison was 1.5×10^{-5} and the least significant was 6×10^{-5} . When we applied this cutoff to the microarray data, the t test returned >500 gene pairs with higher significance (Fig. 1B) with p values up to 1×10^{-15} . All data were run on raw, normalized and logged data for comparison. To establish the false discovery rate, and the level of significance that should be applied to relieve the effects of false discovery, we ran a t test on a randomly generated set of 29 (31042×31042) matrices (the same size as the experimental data matrices). We then applied these thresholds to our raw, normalized and logged data for comparison between these types.

Network inference using the Glasso algorithm

The Glasso algorithm is based on determining an estimated precision matrix. This precision matrix is the inverse of the estimated sample covariance matrix, derived from data. For two features, a zero component of the precision matrix would mean the corresponding variance is infinite, i.e., that the correlation is uniform and infinitely spread, and the features are therefore totally uncorrelated. In our case these features can be viewed as nodes, representing genes or expression sites generally, in a network and the method is determining dependencies of expression levels. With the Glasso algorithm a penalty term is used to force components of the estimated precision matrix toward zero. Those components of the precision matrix which remain non-zero correspond to the highest interdependencies between nodes (e.g., genes) in the network.

The Glasso algorithm has various advantages over other algorithms for network inference. It is one of the fastest network inference algorithms available, running 30–4000 times faster than its competitors (Friedman et al., 2008). It can manage large amounts of data, running on $1000 \times$

1000 matrices in around a minute and the use of an L1 (Lasso) penalty term to enforce sparsity enables few key functional links to be inferred from large amounts of data. This fitted our problem well as we wish to obtain a few high-probability links to test experimentally from a large amount of data.

Glasso estimates a sparse undirected graph by applying an L1 penalty to the estimation of an inverse covariance matrix. The model assumes that data (in this case, gene expression data) is continuous and that the observations comes from a multivariate Gaussian distribution, that has mean μ and covariance matrix Σ . This covariance matrix encodes the extent that gene expression values are correlated and therefore its components give a measure of strength of correlation. As such the matrix is symmetrical along its diagonal. An estimation of the inverse of the covariance matrix, called the estimated precision matrix, is used to infer potential links.

To determine those features which are most interdependent Glasso uses a penalty term in the algorithm to force components of the estimated precision matrix to zero. A parameter ρ , prefacing this penalty term, controls the extent of sparsity in the estimated network. Those remaining components of the precision matrix which remain non-zero correspond to the highest interdependencies among nodes (genes) in the network. Let S be the sample covariance matrix and S^{-1} be its inverse. Let Γ be the estimated precision matrix. The objective function of the Glasso algorithm has two terms, which are optimized via an algorithm. The first term is of the form $KL[N(0, \Gamma), N(0, S^{-1})]$, where KL is the Kullback-Leibler divergence, a measure of similarity of distributions, and $N(0, M)$ is a Gaussian distribution with a zero mean vector and precision matrix M . Minimization of this term would therefore enhance the similarity of the estimated precision matrix Γ to the inverse sample covariance matrix. The second term in the objective function is $\rho \|\Gamma\|_1$ where $\|\Gamma\|_1$ is the sum of the absolute values in Γ . Minimization of this term will force the values of the components within Γ to zero. Effectively then, the algorithm tries to move Γ as closely as possible toward S^{-1} subject to the influence of the second term, which is trying to force component values within the matrix Γ toward zero, the relative influence of these two terms controlled by ρ . Those remaining components of the precision matrix which remain non-zero correspond to the highest interdependencies among nodes in the network.

The sample covariance matrix becomes singular when the dimension of the matrix is much larger than the sample size. For this reason, to model large covariance matrices, the usual approximation is via a sparse estimation matrix, with most entries zero (Bickel and Levina, 2008). This is the route taken by the Glasso algorithm, in which optimization of a norm-1 penalized maximum likelihood leads to a sparse estimation of the precision matrix (Friedman et al., 2008). To further understand this issue we used the F07AGF routine of the Numerical Algorithms Group (NAG) Library (Mark 24) to determine the condition number μ of the matrices used in our study. Approximately, if we determine that the condition number μ to be

of order $1.0E+k$ then k digits of numerical accuracy would be lost due to accumulated arithmetical loss of precision (Cheney and Kincaid, 2007). For our dataset with 500 features (representing genes), the NAG routine gives a condition number of $0.69E+15$ for the sample covariance matrix. Hence, the data-derived covariance matrix itself is close to being rank-deficient (though no covariance matrix inversion or other data manipulations are required by the method). For the least sparse approximation we used in our numerical experiments, the estimated condition number of the sparse precision matrix was $7.17E+5$, suggesting numerical accuracy was satisfactory for the given machine precision. However, this issue of the condition number required us to use the subset of 500 genes, rather than the full set of genes.

Using a sample covariance matrix derived from the data, Glasso iteratively derives an estimated inverse covariance matrix (precision matrix). The algorithm uses an L1-norm penalty to drive elements in this precision matrix toward 0. This penalty therefore determines the sparsity of the estimated precision matrix and hence the sparsity of the network of assumed dependencies. This penalty term is prefaced by a parameter ρ and the higher the value of ρ , the greater the sparsity. To find an appropriate value for ρ we chose the known links and non-links of a well-studied pathway, to give an indication of the correct network sparsity, and best choice for ρ . The ERK pathway data evaluated (Sachs et al., 2002) consists of 11 proteins and 11943 observations of their expression levels from 12 perturbation experiments. The ERK pathway is very well studied and a full network of directional links is known for the network. We downloaded the Glasso software (from <http://statweb.stanford.edu/~tibs/gllasso/>) and applied it to this dataset. Setting the Glasso sparsity parameter to $\rho = 4$ gave those links and non-links which have been found in the ERK pathway (Sachs et al., 2002).

In addition to running Glasso on the top 500 differentially expressed genes, a Pearson correlation measure was also derived from the data. The genes pairings returned by Glasso were in the top most highly correlated pairings as determined by the Pearson correlation coefficient.

Animal experiment

All experiments were performed under a Home Office United Kingdom license held under, and in strict accordance with, the provisions of the United Kingdom Animals (Scientific Procedures) Act (1986); they were also approved by the local Animal Welfare and Ethical Review Board. Twelve-week-old male SD Rats (Harlan) were given access to standard laboratory rat chow and water ad libitum for one week to acclimatize to laboratory conditions, following which half the animals were completely deprived of drinking water for 72 h (dehydration), which elicits a reliable and consistent increase in plasma osmolality with limited weight loss (Greenwood et al., 2015). Animals were killed by stunning and then decapitated with a small animal guillotine (Harvard Apparatus). The brain was quickly extracted and placed on aluminum foil and frozen with dry ice. Brains were stored at -80°C .

Table 1. List of primers used for qRT-PCR

Gene	GenBank	Primers
<i>Caprin2</i>	AI412606	Forward CAGGGTTAAGTGCAAGCGAT Reverse CTGGTGGTTGACTGGTTGAG QuantiTect primer assay; Rn_Atf4_1_SG: QT00366233
<i>Atf4</i>	NM_024403	Forward GCCCAAAGGCCTTCATCATT Reverse CCCCCCTTCTGCTTGTCTA QuantiTect primer assay; Rn_Hbb_1_SG: QT00394107
<i>Hbb</i>	BI287300 NM_033234	Forward CGACTGACAGGGACTCATCA Reverse ATGGGACAGGCCAAAGAAGA Forward CGCGTGTGCCACCTTATTTA Reverse CCAAACAGCTAAATATGCAAGTCC
<i>Opn3</i>	BI289640	Forward TCAGGAGATAATGATGGGCAGA Reverse CCCCACTAGGACTGTGATCC
<i>Ran</i>	NM_053439	Forward AACCTGTACCTCCGTTCCCTG Reverse CCCAAGCCTGTACCCAGTAT
<i>Pcp4</i>	NM_013002	Forward CCAGCCCCATCTCCTTAACCT Reverse AGACTGTTCCCCCTCGGTAT
<i>Igfbp2</i>	NM_013122	Forward ACCAATGCCACTTTGCTTCA Reverse CTGCCTAGTCGTGCGGAAGTC
<i>Pdyn</i>	BF412731	Forward GGATCCTCTGGTGACCTTT Reverse CTGTTTCTTCTTGCCACCCC
<i>Ap1s2</i>	AI045228	Forward AGGATGTCTCTCCTGGAAGC Reverse TTGTTAGCACACGGAACACTT
<i>Atp1a2</i>	NM_012505	Forward GCACTGTTGAAACCTCCCTC Reverse TGACGAGCAACTTGGATGTTT
<i>Hmgn2</i>	BM391736	Forward AATCTTCCCCCAGCAGTTCTT Reverse CACTATAGGGAATTTGGCCCTC
<i>Gja1</i>	AI411352	Forward ATCTCCAAGGTGGTGGGAAG Reverse AAAGTGGGTGTGGATCCTGT
<i>Hba1</i>	AI179404	Forward GCGTCTGCAGCCATGAGTA Reverse TGGCATTGGCGATTTCGTTG
<i>EST</i>	AI577319	
<i>Rpl19</i>	NM_031103.1	

Functional validation of the Glasso-derived gene network

The rat adrenal pheochromocytoma cell line (PC12) was grown complete DMEM (Sigma D6546) containing 10% (v/v) horse serum (HS; Gibco 16050), 5% (v/v) heat-inactivated fetal bovine serum (Gibco 10500), 1% (v/v) penicillin/streptomycin solution (Pen Strep; Gibco 15140), and 2 mM L-glutamine (Gibco 25030). Cells were cultured onto tissue culture flasks precoated with 40 μ g/ml rat-tail Type I collagen (Type VII, C8897, Sigma Aldrich) and maintained at 37°C in a humidified incubator with 5% (v/v) CO₂. On reaching confluence, cells were passaged and plated onto collagen-coated 12-well tissue culture plates with complete DMEM as described above. Differentiation of PC12 cells was initiated by replacing the medium with serum-free DMEM containing 0.25% (w/v) bovine serum albumin (Sigma A17906), 1% (v/v) HS, 1% (w/v) Pen Strep solution, and 50 ng/ml nerve growth factor (Life Technologies13257-019). Medium and NGF were replaced every 2 d. At day 4 of NGF treatment, *Caprin2* shRNA lentivirus was added to the medium, with a scrambled shRNA lentivirus being used as a control. Lentiviral vectors containing shRNA of *Caprin2* and scrambled shRNA control were produced as previously described (Konopacka et al., 2015). For overexpression studies of *Caprin2* in PC12 cells, an adenovirus expressing full-length *Caprin2* cDNA (Konopacka et al., 2015) was used, with an eGFP-expressing virus as a control. Production of adenoviral vectors has been described (Greenwood et al., 2015).

qRT-PCR

Tissue from SON was sampled using a cryostat, taking 60- μ m coronal slices, and the SON was punched using a 0.5-mm tissue punch (Interfocus). Twelve punches were taken from the left and right SON (24 total per brain) and stored on dry ice in 1.5-ml tubes. Total RNA was extracted from punched samples by combining TRIzol reagent with Qiagen RNeasy kit protocols (Qiagen). The punched samples were removed from dry ice and rapidly resuspended, by vortexing, in 1-ml TRIzol reagent. Following TRIzol phase separation with chloroform, 350 μ l of the upper aqueous phase was removed, mixed with 350- μ l 70% (v/v) ethanol and applied to RNeasy columns. The remaining steps were performed as recommended by the manufacturer. For cell studies, cells were collected and lysed with 350- μ l TRIzol reagent on day 7 after NGF treatment (3 d after virus transduction). RNA extraction was performed using Direct-Zol RNA Mini Prep Kit (Zymo Research) following the manufacturer's instructions. RNA was converted to cDNA using QuantiTect Reverse Transcription kit (Qiagen). Primers for qPCR were designed using the NCBI PrimerBLAST tool (<http://www.ncbi.nlm.nih.gov/tools/primer-blast/>; Table 1). Note that the primer set for *Hbb* used for the analysis of Sprague Dawley (SD) SON RNA (derived from sequence BI287300) did not detect PC12 transcripts, presumably due to that cell line being derived from a different strain of rat. We therefore used primers designed to detect all rat *Hbb* alleles. PCRs were performed on ABI7500 or StepOnePlus Real-time PCR Systems (Applied Biosystem) using FastStart Univer-

sal SYBR Green Master Mix (Roche). The housekeeping gene *Rpl19* was used to normalize expression from targets and to calculate $2^{-\Delta\Delta C_T}$ (Livak and Schmittgen, 2001) to analyze the relative change in gene expression.

Statistical tests

Statistical differences between two experimental groups were evaluated using independent-sample unpaired Student's *t* tests; $p < 0.05$ was considered significant.

Results

Significance testing of microarray data

Transcriptome datasets were derived from Affymetrix oligonucleotide array analysis of that the SD rat SON subject to three physiologic transitions that elicit functional plasticity, namely dehydration in both males (Hindmarch et al., 2006) and females (Qiu et al., 2011), salt-loading in males (Greenwood et al., 2015), and lactation in females (Qiu et al., 2011). To avoid the false discovery inherent in large comparisons, we employed a two-sample *t* test with a 31042×29 matrix of randomly generated data (see Methods) and established an appropriate significance threshold of $n \times 10^{-5}$. We selected the top 500 genes that were regulated in the SON between naïve and plastic states that satisfied the significance threshold (all *p* values $< 1 \times 10^{-15}$) and used these to establish the 500×500 covariance matrix computed and solved by Glasso.

Network reconstruction using Glasso and Pearson

Running Glasso with a L1 penalty parameter of 30 and ignoring links below a threshold of 0.0001 yielded 28 unique genes (Table 2) engaged in 48 links (Table 3). Pearson correlation returned 47 unique genes (Table 4) engaged in 32 bidirectional links with a correlation measure over 0.95 between (Table 5). We filtered these results to find those genes which had a high fan-out in terms of connectivity to other genes. We established subsets of genes with either a fan-out of more than one link, or at least one link to another gene with a fan-out greater than one. This resulted in networks of 14 genes from the Glasso reconstruction (Fig. 2A) and seven genes from the Pearson correlation (Fig. 2B). Only one gene satisfied these requirements in both networks; *Caprin2* was ranked 50th overall in the *t* test.

qRT-PCR validation

We validated the expression profiles of the 14 genes identified by Glasso using qRT-PCR of RNA extracted from euhydrated and dehydrated 12-week-old male SD SON ($n = 10$ for euhydrated and $n = 11$ for dehydrated). Of the original 14 genes in the Glasso network (Fig. 2A), 10 had significantly different ($p < 0.05$) relative expression levels (Fig. 3), while three of the predicted genes were false positives and were therefore excluded (*Hmgn2*, BM391736; *Gja1*, AI411352; *Hba1*, AI179404). Primer sets for one of the expressed sequence tags (ESTs) AI577319 failed to deliver data. To establish whether correlations exist between the genes validated by qRT-PCR a Pearson

Table 2. List of unique genes in the Glasso network

1367576_at	S41066	<i>Gpx1</i>
1367590_at	NM_053439	<i>Ran</i>
1367624_at	NM_024403	<i>Atf4</i>
1367648_at	NM_013122	<i>Igfbp2</i>
1367681_at	NM_022523	<i>CD151</i>
1367887_at	NM_017024	<i>Lcat</i>
1368145_at	NM_013002	<i>Pcp4</i>
1368170_at	NM_024371	<i>Slc6a1</i>
1368565_at	NM_019225	<i>Slc1a3</i>
1370172_at	AA892254	<i>Sod2</i>
1370240_x_at	AI179404	<i>Hba1</i>
1370442_at	U25684	<i>Tmsb11</i>
1371245_a_at	BI287300	<i>Hbb</i>
1371352_at	BM391736	<i>Hmgn2</i>
1372002_at	AI411352	<i>Gja1</i>
1373260_at	AI412606	<i>Caprin2</i>
1375856_at	AI102258	<i>EST</i>
1386911_at	NM_012505	<i>Atp1a2</i>
1388608_x_at	AI577319	<i>EST</i>
1388795_at	AI101500	<i>EST</i>
1389586_at	BE107169	<i>EST</i>
1398888_at	AI408819	<i>H3f3b</i>
1383294_at	BF412731	<i>Pdyn</i>
1393263_at	AW522530	<i>Snhg11</i>
1393373_at	BI289640	<i>Opn3</i>
1394940_at	BI294811	<i>Fam46a</i>
1395249_at	BF400750	<i>Snhg11</i>
1398616_at	AI045228	<i>Ap1s2</i>

Column 1, Affymetrix probe ID; column 2, GenBank accession number; column 3, current gene ID.

correlation was performed which resulted in 8 out of 10 correlations (Fig. 4).

Functional validation of the Glasso network *in vitro*

We developed an *in vitro* model to assess the functional validity of the Glasso predicted network. Rat adrenal pheochromocytoma PC12 cells can be made to differentiate into cells with a neurone-like phenotype by treatment with nerve growth factor (NGF). First, we used qRT-PCR to show that transcripts encoded by a sub-set of the genes of the Glasso network are expressed in PC12 cells, and that their expression level is changed following NGF treatment (Fig. 5). This analysis revealed that all the genes in the network, except Prodynorphin (*Pdyn*) and ATPase Na⁺/K⁺ transporting subunit- $\alpha 2$ (*Atp1a2*), are expressed in undifferentiated PC12 cells. Expression of *Pdyn* mRNAs are dramatically increased in NGF-treated cells (>100,000-fold increase), while the level of *Atp1a2* remains undetectable. The expression of *Caprin2*, Opsin-3 (*Opn3*), and Purkinje cell protein 4 (*Pcp4*) transcripts is decreased in PC12 cells following NGF treatment (*Caprin2* 0.425, $p = 0.006$; *Opn3* 0.343, $p = 0.017$; *Pcp4* 0.052, $p = 0.003$), while Ras oncogene family member *Ran*, insulin-like growth factor-binding protein 2 (*Igfbp2*), activating transcription factor 4 (*Atf4*), hemoglobin subunit- β (*Hbb*) and adaptor-related protein complex 1 $\sigma 2$ -subunit (*Ap1s2*) mRNA abundance are not significantly changed.

We then manipulated the expression of nodal gene *Caprin2* in differentiated PC12 cells using lentiviral vectors that express either an shRNA specific for all splice iso-

Table 3. Glasso pairs

1383294_at	BF412731	1367624_at	NM_024403	1383294_at	BF412731	1371245_a_at	BI287300
1373260_at	AI412606	1367624_at	NM_024403	1373260_at	AI412606	1371245_a_at	BI287300
1386911_at	NM_012505	1367624_at	NM_024403	1386911_at	AI179404	1371245_a_at	BI287300
1370240_x_at	AI179404	1367624_at	NM_024403	1386911_at	AI577319	1371245_a_at	BI287300
1373260_at	AI412606	1371352_at	BM391736	1386911_at	NM_012505	1375856_at	AI102258
1370240_x_at	AI179404	1371352_at	BM391736	1373260_at	AI412606	1370172_at	AA892254
1367624_at	NM_024403	1383294_at	BF412731	1367624_at	NM_024403	1386911_at	NM_012505
1373260_at	AI412606	1383294_at	BF412731	1383294_at	BF412731	1386911_at	NM_012505
1372002_at	AI411352	1383294_at	BF412731	1367590_at	NM_053439	1386911_at	NM_012505
1398616_at	AI045228	1383294_at	BF412731	1368145_at	NM_013002	1386911_at	NM_012505
1367648_at	NM_013122	1383294_at	BF412731	1368565_at	NM_019225	1386911_at	NM_012505
1371245_a_at	BI287300	1383294_at	BF412731	1372002_at	AI411352	1386911_at	NM_012505
1386911_at	NM_012505	1383294_at	BF412731	1368170_at	NM_024371	1386911_at	NM_012505
1370240_x_at	AI179404	1383294_at	BF412731	1367648_at	NM_013122	1386911_at	NM_012505
1388608_x_at	AI577319	1383294_at	BF412731	1375856_at	AI102258	1386911_at	NM_012505
1373260_at	AI412606	1367590_at	NM_053439	1367624_at	NM_024403	1370240_x_at	AI179404
1386911_at	NM_012505	1367590_at	NM_053439	1371352_at	BM391736	1370240_x_at	AI179404
1373260_at	AI412606	1368145_at	NM_013002	1383294_at	BF412731	1370240_x_at	AI179404
1386911_at	NM_012505	1368145_at	NM_013002	1368145_at	NM_013002	1370240_x_at	AI179404
1370240_x_at	AI179404	1368145_at	NM_013002	1373260_at	AI412606	1370240_x_at	AI179404
1367624_at	NM_024403	1373260_at	AI412606	1393373_at	BI289640	1370240_x_at	AI179404
1371352_at	BM391736	1373260_at	AI412606	1367681_at	NM_022523	1370240_x_at	AI179404
1383294_at	BF412731	1373260_at	AI412606	1398616_at	AI045228	1370240_x_at	AI179404
1367590_at	NM_053439	1373260_at	AI412606	1393263_at	AW522530	1370240_x_at	AI179404
1368145_at	NM_013002	1373260_at	AI412606	1371245_a_at	BI287300	1370240_x_at	AI179404
1367887_at	NM_017024	1373260_at	AI412606	1388608_x_at	AI577319	1370240_x_at	AI179404
1393373_at	BI289640	1373260_at	AI412606	1383294_at	BF412731	1388608_x_at	AI577319
1389586_at	BE107169	1373260_at	AI412606	1373260_at	AI412606	1388608_x_at	AI577319
1394940_at	BI294811	1373260_at	AI412606	1398616_at	AI045228	1388608_x_at	AI577319
1398888_at	AI408819	1373260_at	AI412606	1371245_a_at	BI287300	1388608_x_at	AI577319
1370442_at	U25684	1373260_at	AI412606	1370240_x_at	AI179404	1388608_x_at	AI577319
1367576_at	S41066	1373260_at	AI412606	1373260_at	AI412606	1388795_at	AI101500
1372002_at	AI411352	1373260_at	AI412606	1373260_at	AI412606		
1398616_at	AI045228	1373260_at	AI412606				
1367648_at	NM_013122	1373260_at	AI412606				
1395249_at	BF400750	1373260_at	AI412606				
1371245_a_at	BI287300	1373260_at	AI412606				
1370172_at	AA892254	1373260_at	AI412606				
1370240_x_at	AI179404	1373260_at	AI412606				
1388608_x_at	AI577319	1373260_at	AI412606				
1388795_at	AI101500	1373260_at	AI412606				
1373260_at	AI412606	1367887_at	NM_017024				
1373260_at	AI412606	1393373_at	BI289640				
1370240_x_at	AI179404	1393373_at	BI289640				
1373260_at	AI412606	1389586_at	BE107169				
1373260_at	AI412606	1394940_at	BI294811				
1373260_at	AI412606	1398888_at	AI408819				
1373260_at	AI412606	1370442_at	U25684				
1386911_at	NM_012505	1368565_at	NM_019225				
1373260_at	AI412606	1367576_at	S41066				
1370240_x_at	AI179404	1367681_at	NM_022523				
1383294_at	BF412731	1372002_at	AI411352				
1373260_at	AI412606	1372002_at	AI411352				
1386911_at	NM_012505	1372002_at	AI411352				
1386911_at	NM_012505	1368170_at	NM_024371				
1383294_at	BF412731	1398616_at	AI045228				
1373260_at	AI412606	1398616_at	AI045228				
1370240_x_at	AI179404	1398616_at	AI045228				
1388608_x_at	AI577319	1398616_at	AI045228				
1383294_at	BF412731	1367648_at	NM_013122				
1373260_at	AI412606	1367648_at	NM_013122				
1386911_at	NM_012505	1367648_at	NM_013122				
1370240_x_at	AI179404	1393263_at	AW522530				
1373260_at	AI412606	1395249_at	BF400750				

List of the pairs which retained a covariance value >0.0001 , i.e., potential links. Columns 1 (Affymetrix probe ID) and 2 (GenBank accession number) are the first gene, columns 3 (Affymetrix probe ID) and 4 (GenBank accession number) are the second gene. Note that the list contains duplicates, so although it is 96 long, there are 48 links.

forms of *Caprin2* (Konopacka et al., 2015) to knockdown endogenous expression (Fig. 6A), or an Adenoviral vector expressing full-length rat *Caprin2* cDNA (Konopacka et al., 2015) to elicit overexpression (Fig. 6B). We then used qRT-PCR to ask about the effects of *Caprin2* knockdown (Fig. 6C) or overexpression (Fig. 6D) on the levels of transcripts encoded by putative target genes within the Glasso network. With the exception of the *Atf4* and *Igfbp2* mRNAs, the expression of which was not altered by manipulation of *Caprin2*, knockdown or overexpression of *Caprin2* *in vitro* had opposite effects on *Pdyn*, *Opn3* and *Hbb* mRNA abundance. Thus, while *Caprin2* knockdown increased *Pdyn* mRNA levels (3.833, $p = 0.00004$), *Caprin2* overexpression decreased *Pdyn* transcript abundance (0.572, $p = 0.035$). In contrast, both *Opn3* and *Hbb* levels were decreased by *Caprin2* knockdown (*Opn3* 0.477, $p = 0.00004$; *Hbb* 0.323, $p = 0.0013$), but were increased following *Caprin2* overexpression (*Opn3* 1.506, $p = 0.0023$; *Hbb* 2.771, $p = 0.0008$).

Discussion

Following stimulatory physiologic cues, such as dehydration, salt-loading and lactation, the SON of the hypothalamus undergoes a function related plasticity that has previously been described in the rat at the transcriptome

Table 4. List of unique genes in the Pearson network

1367624_at	NM_024403	<i>Atf4</i>
1367648_at	NM_013122	<i>Igf1bp2</i>
1367654_at	NM_031819	<i>Fat1</i>
1367660_at	NM_024162	<i>Fabp2</i>
1368170_at	NM_024371	<i>Slc6a1</i>
1368559_at	NM_017091	<i>Pcsk1</i>
1370030_at	NM_017305	<i>Gclm</i>
1370240_x_at	AI179404	<i>Hba1</i>
1370442_at	U25684	<i>Tmsb1l</i>
1370575_a_at	D50734	<i>Azin1</i>
1371433_at	BM384999	EST
1372754_at	BG666424	<i>Appl2</i>
1373092_at	BE109587	<i>Tgfb3</i>
1373260_at	AI412606	<i>Caprin2</i>
1373380_at	AI169085	EST
1373699_at	BM391164	EST
1373870_at	BE110630	<i>Fam98a</i>
1374004_at	BM387902	<i>Prepl</i>
1374709_at	AI406795	<i>Hlf</i>
1374812_at	AA818197	<i>Ptpn13</i>
1374941_at	BF397951	EST
1375856_at	AI102258	EST
1375964_at	BF282282	<i>Psp1</i>
1376836_at	BF419655	EST
1387037_at	AF022247	<i>Cubn</i>
1388145_at	BM390128	<i>Tnxa-psq</i>
1388608_x_at	AI577319	<i>Hba1</i>
1388770_at	BI275670	<i>Ufm1</i>
1388795_at	AI101500	EST
1389020_at	BM389149	EST
1389135_at	AW140637	<i>Ctsp2</i>
1398348_at	AA945604	EST
1377725_at	AI575322	EST
1378320_at	BG373845	<i>Rlb1</i>
1379566_at	AW527929	<i>Rbm11</i>
1379900_at	AI043697	<i>Aldh5a1</i>
1382008_at	AI044348	<i>Rnls</i>
1382021_at	AA850650	<i>Pkd2</i>
1382905_at	AI102514	<i>Mrc2</i>
1383413_at	AW531481	<i>Hhat1</i>
1391923_at	BG376838	EST
1392108_at	BF390648	<i>RM2</i>
1393165_at	BG377684	<i>Tmem206</i>
1393373_at	BI289640	<i>Opn3</i>
1393837_at	AI145227	EST
1394029_at	BF283049	<i>Vma21</i>
1398616_at	AI045228	<i>Ap1s2</i>

Column 1, Affymetrix probe ID; column 2, GenBank accession number; column 3, current gene ID.

level (Hindmarch et al., 2006; Qiu et al., 2011; Greenwood et al., 2015). Using the unsupervised Glasso algorithm (Friedman et al., 2008), we sought to reconstruct a putative network from 500 plastic SON genes in which genes are the nodes and the edges are the inferred interactions. The most active nodal gene identified within the network was RNA-binding protein *Caprin2*. To test the validity of the Glasso approach, we sought an *in vitro* cell culture model in which genes of the predicted network are expressed. We found that differentiated PC12 cells met these criteria. We then either overexpressed or knocked down *Caprin2* transcripts in differentiated rat pheochromocytoma PC12 cells, and showed that these manipula-

Table 5. Pearson pairs

1367624_at	NM_024403	1374941_at	BF397951
1374941_at	BF397951	1367624_at	NM_024403
1391923_at	BG376838	1373260_at	AI412606
1398616_at	AI045228	1373260_at	AI412606
1370575_a_at	D50734	1373260_at	AI412606
1389135_at	AW140637	1373260_at	AI412606
1382008_at	AI044348	1388770_at	BI275670
1383413_at	AW531481	1377725_at	AI575322
1388770_at	BI275670	1382008_at	AI044348
1370575_a_at	D50734	1393165_at	BG377684
1393837_at	AI145227	1393373_at	BI289640
1373260_at	AI412606	1391923_at	BG376838
1379566_at	AW527929	1391923_at	BG376838
1373380_at	AI169085	1391923_at	BG376838
1370575_a_at	D50734	1391923_at	BG376838
1377725_at	AI575322	1383413_at	AW531481
1382021_at	AA850650	1367654_at	NM_031819
1372754_at	BG666424	1367654_at	NM_031819
1393373_at	BI289640	1393837_at	AI145227
1367660_at	NM_024162	1373870_at	BE110630
1367660_at	NM_024162	1370442_at	U25684
1376836_at	BF419655	1375964_at	BF282282
1394029_at	BF283049	1370030_at	NM_017305
1398348_at	AA945604	1392108_at	BF390648
1374709_at	AI406795	1389020_at	BM389149
1387037_at	AF022247	1374812_at	AA818197
1373092_at	BE109587	1374812_at	AA818197
1370030_at	NM_017305	1394029_at	BF283049
1374812_at	AA818197	1387037_at	AF022247
1373870_at	BE110630	1367660_at	NM_024162
1370442_at	U25684	1367660_at	NM_024162
1391923_at	BG376838	1379566_at	AW527929
1375856_at	AI102258	1368170_at	NM_024371
1368559_at	NM_017091	1374004_at	BM387902
1391923_at	BG376838	1373380_at	AI169085
1374709_at	AI406795	1382905_at	AI102514
1371433_at	BM384999	1382905_at	AI102514
1374004_at	BM387902	1368559_at	NM_017091
1373260_at	AI412606	1398616_at	AI045228
1375964_at	BF282282	1376836_at	BF419655
1388145_at	BM390128	1367648_at	NM_013122
1373699_at	BM391164	1367648_at	NM_013122
1389020_at	BM389149	1374709_at	AI406795
1382905_at	AI102514	1374709_at	AI406795
1373092_at	BE109587	1374709_at	AI406795
1367648_at	NM_013122	1388145_at	BM390128
1373260_at	AI412606	1370575_a_at	D50734
1393165_at	BG377684	1370575_a_at	D50734
1391923_at	BG376838	1370575_a_at	D50734
1392108_at	BF390648	1398348_at	AA945604
1367648_at	NM_013122	1373699_at	BM391164
1382905_at	AI102514	1371433_at	BM384999
1375856_at	AI102258	1379900_at	AI043697
1368170_at	NM_024371	1375856_at	AI102258
1379900_at	AI043697	1375856_at	AI102258
1373260_at	AI412606	1389135_at	AW140637
1374812_at	AA818197	1373092_at	BE109587
1374709_at	AI406795	1373092_at	BE109587
1367654_at	NM_031819	1382021_at	AA850650
1367654_at	NM_031819	1372754_at	BG666424
1388795_at	AI101500	1378320_at	BG373845

1388608_x_at	AI577319	1370240_x_at	AI179404
1370240_x_at	AI179404	1388608_x_at	AI577319
1378320_at	BG373845	1388795_at	AI101500

Pearson correlated pairs with a value >0.95. Columns 1 (Affymetrix probe ID) and 2 (GenBank accession number) are the first gene, columns 3 (Affymetrix probe ID) and 4 (GenBank accession number) are the second gene. Note that the list contains duplicates, so although it is 64 long, there are 32 links.

tions had significant opposite effects on the levels of putative target mRNAs.

A major bottleneck of the “omic” era is the sheer scale and complexity of the datasets, and the resulting daunting problem of identifying suitable targets for often expensive and time consuming physiologic studies. We sought to address this problem in a mammalian homeostatic system that demonstrates functionally important plasticity following the physiologic challenges of dehydration, salt-

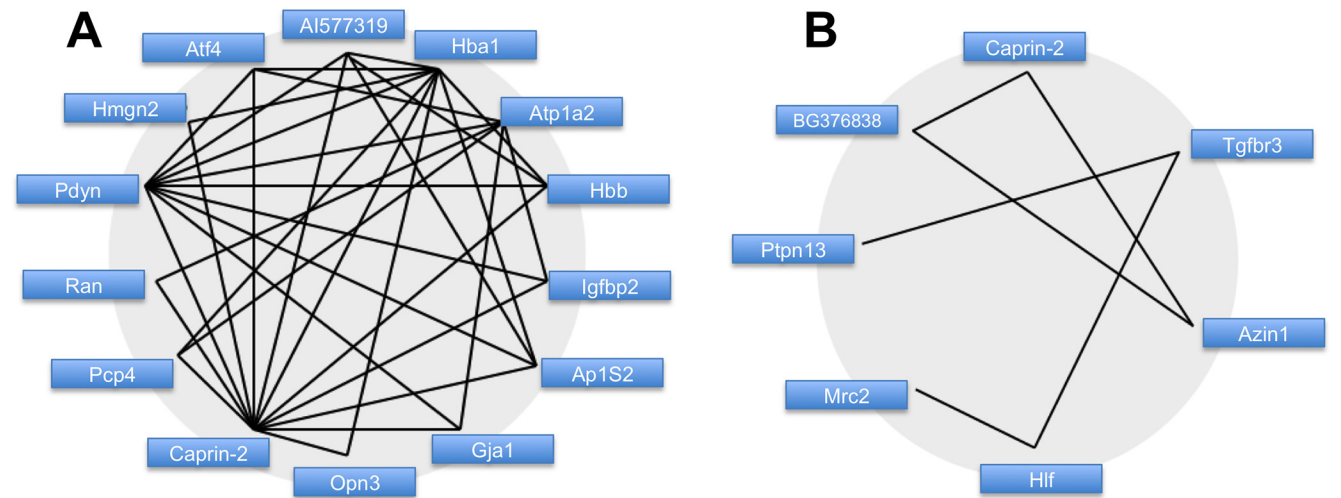


Figure 2. Putative gene networks derived from SON transcriptome data. **A**, The Glasso-derived network. Undirected links are solid black lines. Genes are represented by short names. **B**, The Pearson correlation-derived network. Undirected links are solid black lines. Genes are represented by short names.

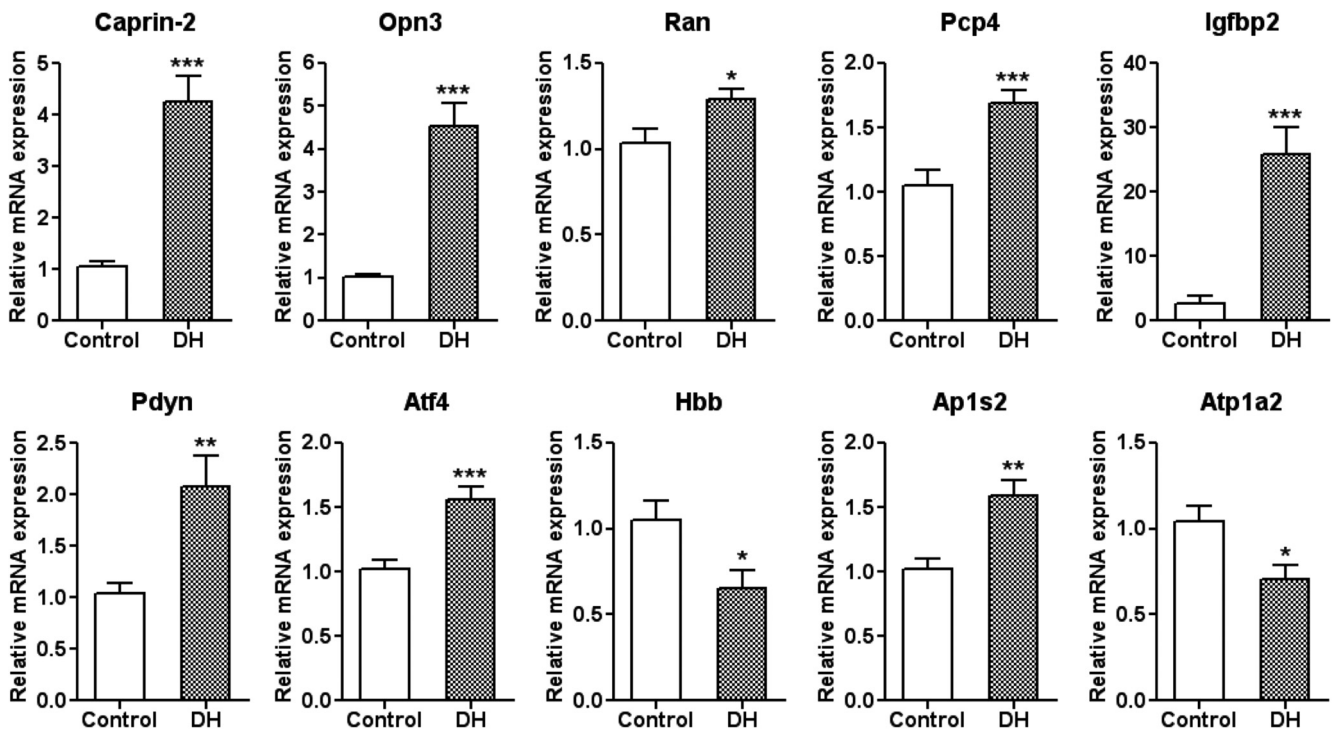


Figure 3. qRT-PCR validation of differential expression. The expression profiles of the 14 genes identified by Glasso were examined by qRT-PCR of RNA extracted from euhydrated (control) and dehydrated (DH) 12-week-old male SD SON. Of the original 14 genes in the Glasso network (Fig. 2A) 10 had significantly different relative expression levels. Error bar, SEM; * $p < 0.05$; ** $p < 0.01$; *** $p < 0.001$; $n = 10$ for control and $n = 11$ for DH.

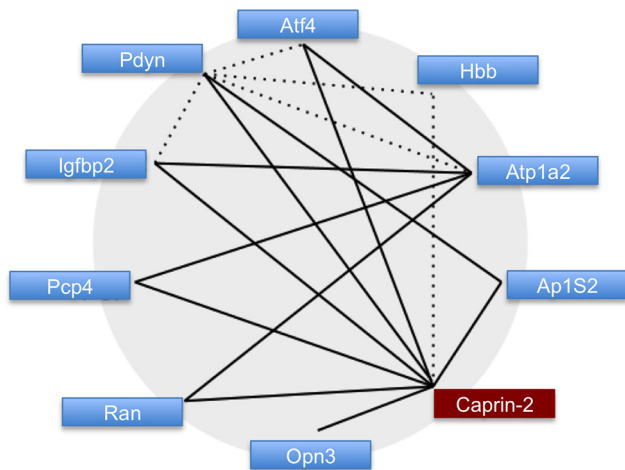


Figure 4. The validated Glasso-derived gene network. Link with significant Pearson correlation ($p < 0.05$) are represented by solid lines. Links not significantly correlated are represented by dotted lines.

loading and lactation. Each of these physiologic challenges activates the SON in a similar manner resulting in a function related plasticity that facilitates an appropriate neuroendocrine response. We hypothesized that there is a common network of genes in this tissue that underpins the general plasticity of the SON. To test this hypothesis, we combined data from the activated plastic SON, e.g., male and female water deprived, male salt-loaded and female lactation, and compared this to the male and female “naïve” data. This comparison resulted in a list of significantly regulated genes on which we performed unsupervised network inference using Glasso to reconstruct a gene network from the SON of the rat hypothalamus in either naïve or physiologically stimulated states, thus al-

lowing us to identify potentially important “hub” genes with high numbers of putative regulatory links (i.e., they have a large fan-out in circo graphs) that may have prominent functional roles. Network inference, while less accurate than supervised methods, is a useful first step in the absence of a training set of known links and non-links. Rather than performing large numbers of perturbation experiments to characterize the entire network, we can use existing microarray data to generate correlations between genes and by applying network inference predict a number of high confidence links, giving us target genes for perturbation experiments, hence maximizing our efforts.

The application of Glasso resulted in a network of 28 genes with 48 links, while Pearson placed 47 genes in a network of 32 links. Only one gene, *Caprin2*, appeared in both networks. To mitigate the false discovery rate further, the network was reduced by eliminating genes below a “richness” criterion. Only those genes that the network infers as having links to at least 2 genes, and that both those genes should be linked to at least two others, were included (Fig. 2). Candidate genes identified from the Glasso inference were then validated by qRT-PCR of SON RNA collected from either euhydrated or dehydrated male rats (Fig. 3). Following elimination of the three genes that did not validate, as well as one that did not deliver data, the remaining genes were subject to Pearson correlation to attempt reengineering of the network (Fig. 4). Examination of this network clearly reveals a central hub gene, *Caprin2*, an RNA-binding protein (Shiina and Tokunaga, 2010) that has been shown to bind the AVP mRNA (Konopacka et al., 2015) and to mediate changes in AVP mRNA abundance and poly(A) tail length (Konopacka et al., 2015). Lentiviral mediated shRNA knockdown of *Caprin2* in the osmotically stimulated hypothalamus shortened the AVP mRNA poly(A) tail and reduced transcript abundance (Konopacka et al., 2015). In an *in vitro* system, *Caprin2* overexpression enhanced the abundance and poly(A) tail length of the AVP mRNA (Konopacka et al., 2015).

To test the physiologic validity of the Glasso network centered on *Caprin2*, we developed an *in vitro* system that enabled us to manipulate *Caprin2* expression and ask about consequential effects on the steady-state levels of putative transcript targets. As the network is based on transcriptome data, the functional links must regulate mRNA abundance. First, we showed that NGF differentiated PC12 cells express all of the genes in the network, except for one (*Atp1a2*; Fig. 5). We then used viral-mediated gene transfer to either knockdown *Caprin2* using a previously characterized specific shRNA (Konopacka et al., 2015), or to overexpress *Caprin2* (Fig. 6). As a consequence, we saw opposite effects on the levels of putative target mRNAs [knockdown (Fig. 6C), overexpression (Fig. 6D)]. Thus, while *Caprin2* knockdown decreased the abundance of *Opn3*, *Ran* and *Hbb* transcripts, overexpression increased the levels of *Opn3* and *Hbb* RNAs. In contrast, *Caprin2* knockdown increased *Pcp4*, *Pdyn*, and *Ap1s2* RNAs, while overexpression decreased *Pdyn* transcript abundance. *Igfbp2* and *Atf4* RNA levels were unaffected by *Caprin2* manipulation.

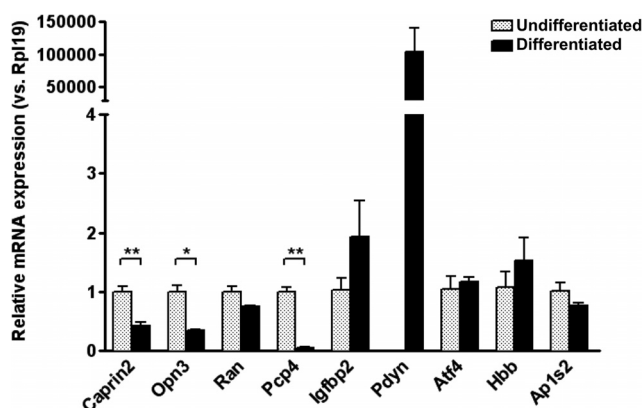


Figure 5. Expression of Glasso network genes in PC12 cells. Relative mRNA expression of genes in the network was examined in both undifferentiated and NGF-treated PC12 cells by qRT-PCR. The relative mRNA level was calculated using $2^{(-\Delta\Delta Ct)}$ method where the expression level of undifferentiated sample was calculated as 1. Since *Pdyn* is undetectable at 40 cycles on qRT-PCR in undifferentiated PC12 cells, the relative mRNA level was calculated by assumption of Ct value of undifferentiated sample as 40 cycles. Error bar, SEM; * $p < 0.05$; ** $p < 0.01$; unpaired Student's *t* test; $n = 3$.

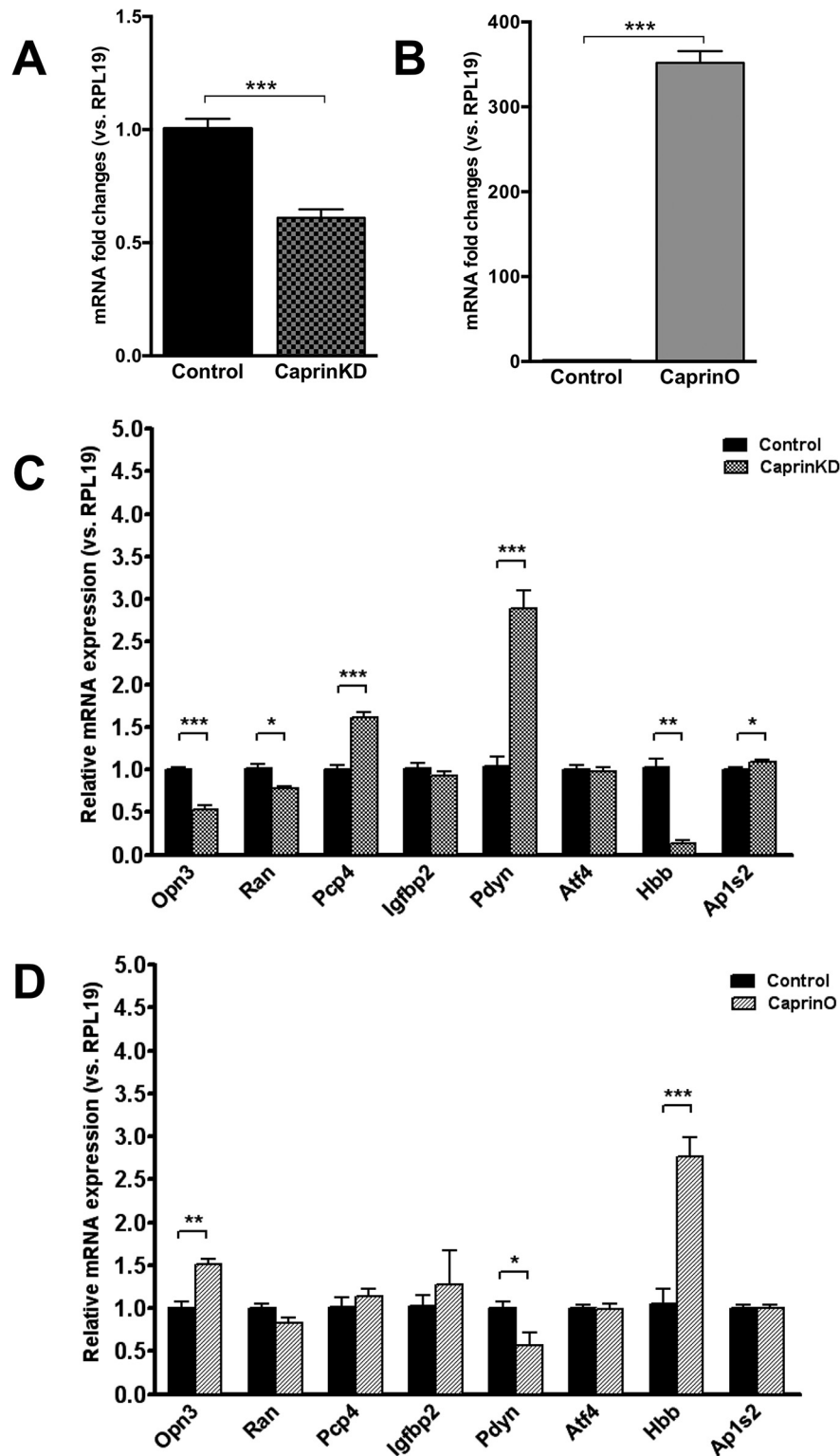


Figure 6. Change in mRNA expression of Glial network genes in differentiated PC12 cells following *Caprin2* knockdown or *Caprin2* overexpression. **A**, For knockdown, NGF-treated PC12 cells were transduced with lentiviral vectors expressing either a *Caprin2* shRNA (CaprinKD) or a scrambled shRNA (control). Relative mRNA expression of endogenous *Caprin2* was examined by qRT-PCR. The relative mRNA level was calculated using $2^{(-\Delta\Delta ct)}$ method, where the expression level of control sample was calculated as 1. Error bar, SEM; *** $p < 0.001$; unpaired Student's t test; $n = 6$. **B**, For overexpression, NGF-treated PC12 cells were transduced with adenoviral vectors expressing either *Caprin2* (CaprinO) or *eGFP* (control). Relative mRNA expression of endogenous *Caprin2* was examined by qRT-PCR. The relative mRNA level was calculated using $2^{(-\Delta\Delta ct)}$ method where the expression level of control sample was calculated as 1. Error bar, SEM; *** $p < 0.001$; unpaired Student's t test; $n = 4$. **C**, NGF-treated PC12 cells were transduced with

continued

lentiviral vectors expressing either a *Caprin2* shRNA (CaprinKD) or a scrambled shRNA (control). Relative mRNA expression of genes in the network was examined by qRT-PCR. The relative mRNA level was calculated using $2^{-(\Delta\Delta Ct)}$ method where the expression level of control sample was calculated as 1. Error bar, SEM; * $p < 0.05$; ** $p < 0.01$; *** $p < 0.001$; unpaired t test; $n = 6$. **D**, NGF-treated PC12 cells were transduced with adenoviral vectors expressing either *Caprin2* (CaprinO) or *eGFP* (control). Relative mRNA expression of genes in the network was examined by qRT-PCR. The relative mRNA level was calculated using $2^{-(\Delta\Delta Ct)}$ method where the expression level of control sample was calculated as 1. Error bar, SEM; * $p < 0.05$; ** $p < 0.01$; *** $p < 0.001$; unpaired Student's t test; $n = 4$.

In the dehydrated SON, an increase in *Caprin2* mRNA expression is accompanied by an increase in the abundance of *Opn3*, *Ran*, *Pcp4*, *Igfbp2*, *Pdyn*, *Atf4*, and *Ap1s2* transcripts, but a decrease in *Hbb* mRNA abundance. Consistent with this, the decrease in *Caprin2* expression following differentiation of PC12 cells reduces *Opn3* and *Pcp4* transcript levels. However, *Pdyn* levels dramatically increase as a consequence of NGF-mediated differentiation of PC12, probably as a consequence of a separate *Caprin2*-independent transcriptional mechanism. We then manipulated *Caprin2* activity in differentiated PC12 cells by overexpression or shRNA-mediated knockdown to ask about effects on the expression on putative network interacting genes. In some cases, we saw dramatic opposite effects. Thus, *Caprin2* knockdown reduced *Opn3* and *Hbb* mRNA levels, but increased *Pdyn* transcript abundance, whereas *Caprin2* overexpression increased *Opn3* and *Hbb* mRNA levels, but reduced *Pdyn* transcript abundance. These data suggest that *Caprin2* functions to increase *Opn3* and *Hbb* expression, but to decrease *Pdyn* expression. These data are consistent with the increased *Opn3* mRNA abundance seen in the dehydrated SON, perhaps through direct association and consequent stabilisation. However, this is contrary to expectation in terms of *Pdyn*, which has increased expression in the dehydrated SON, and *Hbb*, which has decreased expression in the dehydrated SON. We suggest that any role for *Caprin2* in *Pdyn* and *Hbb* mRNA regulation may not be direct and need to be considered in the context of other, possibly transcriptional, mechanisms.

Our data raise questions regarding the molecular nature and physiologic consequences of the regulatory interactions in the *Caprin2* gene network. *Caprin2* knockdown in the *in vivo* hypothalamus leads to dysfunction of the normal physiologic response to salt loading, an osmotic challenge, which in healthy rats leads to a gradual increase of urine output and fluid intake. *Caprin2* knockdown results in a significant decrease in urine output and fluid intake, and an increase in urine osmolality and plasma AVP levels (Konopacka et al., 2015). We hypothesize that these dramatic physiologic consequences are a sum-total of changes in the expression of the gene products encoded by *Caprin2* target genes. That *Pdyn* is a putative target of *Caprin2* is instructive in this regard. The expression of the endogenous opioid peptide *Pdyn* within the hypothalamus is well known, as is its upregulation following dehydration (Sherman et al., 1986). Dynorphin peptide colocalizes with AVP, and both can be released either from axons or somato-dendritically. At the level of the neural lobe, dynorphin is coreleased with AVP and acts on axon terminal κ -opiate receptors to inhibit elec-

trically evoked secretion of oxytocin (Falke, 1988). Centrally, dendritic release of dynorphin appears to regulate MCN electrical activity (Brown and Bourque, 2004; Brown et al., 2004; Brown et al., 2006). It is thus possible that *Caprin2* mediates some of its physiologic effects through the actions of dynorphin. Interestingly, the *Hbb* gene is expressed in the brain (Ohyagi et al., 1994), and encodes the hemorphins, a family of endogenous nonclassical opioid peptides (Nyberg et al., 1997; Zhao et al., 1997).

Using transcriptome data from the physiologically plastic SON as a model, we have shown that our unbiased network inference strategy, using Glasso, has predictive value, and can “enrich” for functional interactions that can be tested experimentally. The application of Glasso to extensive transcriptome datasets will accelerate the identification of physiologically relevant pathways.

References

- Bickel P, Levina E (2008) Covariance regularization by thresholding. *Ann Stat* 36:2577–2604. [CrossRef](#)
- Breyer MD, Ando Y (1994) Hormonal signaling and regulation of salt and water transport in the collecting duct. *Ann Rev Physiol* 56: 711–739. [CrossRef Medline](#)
- Brown CH, Bourque CW (2004) Autocrine feedback inhibition of plateau potentials terminates phasic bursts in magnocellular neurosecretory cells of the rat supraoptic nucleus. *J Physiol* 557:949–960. [CrossRef Medline](#)
- Brown CH, Ludwig M, Leng G (2004) Temporal dissociation of the feedback effects of dendritically co-released peptides on rhythmogenesis in vasopressin cells. *Neuroscience* 124:105–111. [CrossRef Medline](#)
- Brown CH, Leng G, Ludwig M, Bourque CW (2006) Endogenous activation of supraoptic nucleus kappa-opioid receptors terminates spontaneous phasic bursts in rat magnocellular neurosecretory cells. *J Neurophysiol* 95:3235–3244. [CrossRef](#)
- Burbach JP, Luckman SM, Murphy D, Gainer H (2001) Gene regulation in the magnocellular hypothalamo-neurohypophysial system. *Physiol Rev* 81:1197–1267. [Medline](#)
- Carrazana EJ, Pasioka KB, Majzoub JA (1988) The vasopressin mRNA poly(A) tract is unusually long and increases during stimulation of vasopressin gene expression in vivo. *Mol Cell Biol* 8:2267–2274. [Medline](#)
- Carter DA, Murphy D (1989) Independent regulation of neuropeptide mRNA level and poly(A) tail length. *J Biol Chem* 264:6601–6603.
- Falke N (1988) Dynorphin (1–8) inhibits stimulated release of oxytocin but not vasopressin from isolated neurosecretory endings of the rat neurohypophysis. *Neuropeptides* 11:163–167. [Medline](#)
- Friedman J, Hastie T, Tibshirani R (2008) Sparse inverse covariance estimation with the graphical lasso. *Biostatistics* 9:432–441. [Cross-Ref Medline](#)
- Greenwood M, Mecawi A, Hoe SZ, Mustafa MR, Johnson K, Al-Mahmoud G, Elias L, Paton J, Antunes-Rodrigues J, Gainer H, Murphy D, Hindmarch C (2015) A comparison of physiological and transcriptome responses to water deprivation and salt loading in the rat supraoptic nucleus. *Am J Physiol* 308:R559–R568. [CrossRef](#)

- Hatton GI (1997) Function-related plasticity in hypothalamus. *Annu Rev Neurosci* 20:375–379. [CrossRef](#) [Medline](#)
- Hindmarch C, Yao S, Beighton G, Paton J, Murphy D (2006) A comprehensive description of the transcriptome of the hypothalamo-neurohypophyseal system in euhydrated and dehydrated rats. *Proc Natl Acad Sci USA* 103:1609–1614. [CrossRef](#)
- Hindmarch CC, Franses P, Goodwin B, Murphy D (2013) Whole transcriptome organisation in the dehydrated supraoptic nucleus. *Braz J Med Biol Res* 46:1000–1006. [CrossRef](#) [Medline](#)
- Cheney E, Kincaid D (2007) Numerical mathematics and computing. International student edition. Boston, MA: Cengage Learning.
- Kondo N, Arima H, Banno R, Kuwahara S, Sato I, Oiso Y (2004) Osmoregulation of vasopressin release and gene transcription under acute and chronic hypovolemia in rats. *Am J Physiol* 286:E337–E346.
- Konopacka A, Greenwood M, Loh S-Y, Paton J, Murphy D (2015) RNA binding protein Caprin-2 is a pivotal regulator of the central osmotic defense response. *Elife* 4. [CrossRef](#)
- Livak KJ, Schmittgen TD (2001) Analysis of relative gene expression data using real-time quantitative PCR and the $2^{-\Delta\Delta C(T)}$ method. *Methods* 25:402–408. [CrossRef](#)
- Murphy D, Carter DA (1990) Vasopressin gene expression in the rodent hypothalamus: transcriptional and posttranscriptional responses to physiological stimulation. *Mol Endocrinol* 4:1051–1059. [CrossRef](#)
- Murphy D, Antunes-Rodrigues J, Gainer H (2016) Osmoregulation. In: *Molecular neuroendocrinology: from genome to physiology* (Murphy D, Gainer H, eds), pp 331–354. Holboken, NJ: Wiley-Blackwell.
- Nyberg F, Sanderson K, Glämsta EL (1997) The hemorphins: a new class of opioid peptides derived from the blood protein hemoglobin. *Biopolymers* 43:147–156. [CrossRef](#) [Medline](#)
- Ohyagi Y, Yamada T, Goto I (1994) Hemoglobin as a novel protein developmentally regulated in neurons. *Brain Res* 635:323–327. [Medline](#)
- Qiu J, Hindmarch C, Yao S, Tasker J, Murphy D (2011) Transcriptomic analysis of the osmotic and reproductive remodeling of the female rat supraoptic nucleus. *Endocrinology* 152:3483–3491. [CrossRef](#)
- Sachs K, Gifford D, Jaakkola T, Sorger P, Lauffenburger DA (2002) Bayesian network approach to cell signaling pathway modeling. *Sci STKE* 2002:pe38. [CrossRef](#) [Medline](#)
- Sharman G, Ghorbel M, Leroux M, Beaucourt S, Wong LF, Murphy D (2004) Deciphering the mechanisms of homeostatic plasticity in the hypothalamo-neurohypophyseal system—genomic and gene transfer strategies. *Prog Biophys Mol Biol* 84:151–182. [CrossRef](#)
- Sherman TG, Civelli O, Douglass J, Herbert E, Watson SJ (1986) Coordinate expression of hypothalamic pro-dynorphin and pro-vasopressin mRNAs with osmotic stimulation. *Neuroendocrinology* 44:222–228. [Medline](#)
- Shiina N, Tokunaga M (2010) RNA granule protein 140 (RNG140), a paralog of RNG105 localized to distinct RNA granules in neuronal dendrites in the adult vertebrate brain. *J Biol Chem* 285:24260–24269. [CrossRef](#)
- Theodosios DT, El Majdoubi M, Pierre K, Poulain DA (1998) Factors governing activity-dependent structural plasticity of the hypothalamo-neurohypophysial system. *Cell Mol Neurobiol* 18:285–298. [CrossRef](#)
- Zhao Q, Garreau I, Sannier F, Piot JM (1997) Opioid peptides derived from hemoglobin: hemorphins. *Biopolymers* 43:75–98. [CrossRef](#) [Medline](#)
- Zingg HH, Lefebvre DL, Almazan G (1988) Regulation of poly(A) tail size of vasopressin mRNA. *J Biol Chem* 263:11041–11043. [Medline](#)